













# Synthesis, Physico-Chemical Properties and Theoretical Prediction of Electroanalytical Properties of the Novel Benzo-[b][1,8]-naphthyridine-5(10H)-one and Thione

Volodymyr V. Tkach <sup>1,\*</sup> , Marta V. Kushnir <sup>1</sup> , Lyudmyla O. Omelyanchik <sup>2</sup> ,  
Viktoria I. Gencheva <sup>2</sup> , Yulia Yu. Petrusha <sup>2</sup> , Vira V. Kopiika <sup>2</sup> , Olga V. Luganska <sup>2</sup> ,  
Yana G. Ivanushko <sup>3</sup> , José Inácio Ferrão da Paiva Martins <sup>4</sup> , Jarem R. Garcia <sup>5</sup> ,  
Maria João Monteiro <sup>6</sup> , Petro I. Yagodynets' <sup>1,\*</sup> 

<sup>1.</sup> Chernivtsi National University, 58000, Kotsyubyns'ky Str. 2, Chernivtsi, Ukraine

<sup>2.</sup> Zaporizhzhia National University, 69600, Zhukovsky Str. 66, Zaporizhzhia, Ukraine

<sup>3.</sup> Bukovinian State Medical University, 58001, Teatralna Sq., 9, Chernivtsi, Ukraine,

<sup>4.</sup> Faculty of Engineering of the University of Porto, 4200-465, Rua Dr. Roberto Frias, s/n, Porto, Portugal

<sup>5.</sup> State University of Ponta Grossa, Uvaranas Campus, Av. Gal. Carlos Cavalcanti, 4748, 84030-900, Ponta Grossa, PR, Brazil

<sup>6.</sup> University of Trás-os-Montes and Alto Douro, Quinta de Prados, 5001-801, Folhadela, Vila Real, Portugal

\* Correspondence: [nightwatcher2401@gmail.com](mailto:nightwatcher2401@gmail.com) (V.V.T.), [ved1988mid@rambler.ru](mailto:ved1988mid@rambler.ru) (P.I.Y.);

Scopus Author ID 55758299100

Received: 27.09.2023; Accepted: 12.01.2024; Published: 19.02.2024

**Abstract:** A novel group of heterocyclic compounds with potential biological and electroanalytical activity has been obtained and characterized. The compounds have been obtained by condensative heterocyclization of 2-bromo pyridine with anthranilic acid derivatives. Both of them have been characterized and evaluated as potential monomers and electrode modifiers. It has been shown that the novel compounds and their polymers may serve as excellent carbon electrode modifiers for the electrochemical determination of biologically active compounds.

**Keywords:** heterocyclic compounds; biologically active compounds; azaacridines; conducting polymers; electrochemical sensors; stable steady-state.

© 2024 by the authors. This article is an open-access article distributed under the terms and conditions of the Creative Commons Attribution (CC BY) license (<https://creativecommons.org/licenses/by/4.0/>).

## 1. Introduction

Pyridine, quinoline, and acridine are heterocyclic compounds, possessing derivatives with highly expressed biological activity [1–12] and dyeing properties. It is known that some of the pyridinic derivatives are calcium ion antagonists by blocking the calcium channels and possess radio-protecting, cardio-protecting, hepato-protecting antitumor, antimutagenic, antibacterial, antiprotozoal and hypotensive activities, the reason why they are widely used in medicine, pharmacy, and agriculture. They are also used as dyes and pigments [13–21], some of them fluorescent, and as monomers for conducting polymers for electroanalytical use [22–27].

Nowadays, a search for novel quinolinic biologically active compounds, dyes, and their polymer is caused by the necessity of treatment of neglected tropical diseases (malaria, dengue, chikungunya, zika, etc.), new infectious diseases, like COVID-19, Ebola, analytical detection of other biologically active and environmentally aggressive compounds including chemical warfare agents and environmentally stable food additives [28–35]. For this reason, the goal of

this work is to obtain the novel aza-acridonic and aza-thioacridonic heterocyclic compounds, characterize them, and investigate theoretically their electroanalytical activity in the electrochemical determination of biologically active compounds using dopamine and ascorbic acid as models [36–49]. This investigation will also include analyzing the corresponding mathematical model and comparing their behavior with the behavior of similar compounds in similar systems [47–49].

## 2. Materials and Methods

### 2.1. Experimental.

All the reagents have been commercially acquired from Enamine® (Kyiv) and used as given. IR-spectra has been taken on Bruker Alpha using the KBr pills. The mass spectra were taken using Varian MAT-311A equipment, and the elemental composition of the novel compounds was verified on a Vario EL Cube elemental analyzer using the sulfanilamide standard.

The schematic representation of the synthetic procedures has been described in the Figure 1:

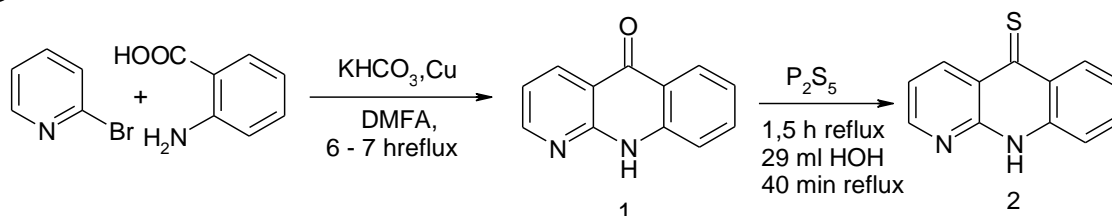


**Figure 1.** Scheme of the synthesis of the compounds.

#### 2.1.1. Benzo[*b*][1,8]naphthyridine-5(10*H*)-one (1) (8-aza-9-acridone).

1,33 g (0,01 mol) of anthranilic acid is dissolved in 50 ml of DMFA, and 1 ml (0,01 mol) 2-bromo-pyridine in 50 ml DMFA, 1,38 g (0,01 mol) of potassium hydrocarbonate and 0,3-0,5 g of reduced copper are added. The mixture is heated and intensively stirred during 6-7 h. Further, the reaction mixture is diluted by hot water and filtered out. The filtrate is acidified by diluted chloridic acid, and the precipitate is filtered out and dried. Yield 1,66 g (85%). The product is obtained as yellow crystalline needles with a melting point of 278-280°C (crystallized from ethanol). Found, %: C – 73,2; H – 4,0; N – 14,1;  $\text{C}_{12}\text{H}_8\text{N}_2\text{O}$ . Calculated, %: C – 73,5; H – 4,1; N – 14,2.

#### 2.1.2. Benzo[*b*][1,8]naphthyridine-5(10*H*)-thione (1) (8-aza-9-thioacridone).

1,96 g (0,01 mol) of the compound (1) is dissolved in 50 ml pyridine, and 1,58 g (0,01 mol) of phosphorus pentasulfide is added. The reaction mixture is heated for 1,5 h. Furthermore, 20 ml of water is added, followed by 30-40 min reflux. The reaction mixture is cooled and diluted with water. The precipitate is filtered out and dried. The product is obtained in the form of yellow needles. Yield 1,86 g (95%). M.P. 162-164 0C (from ethanol). Found, %: C – 67,7; H – 4,0; N – 13,3; S – 15,0.  $\text{C}_{12}\text{H}_8\text{N}_2\text{S}$ . Calculated, %: C – 67,9; H – 3,8; N – 13,2; S – 15,1.

The mechanism of the first reaction is analogous to Ullmann coupling, with the only difference that the coupling is accompanied by heterocyclization with the 4-pyridonic ring closure in the middle of the product due to the enhanced electrophilicity of the 3<sup>rd</sup> position of

the pyridinic ring, activated by bromine atom. 8-aza-9-thioacridone has been obtained for the first time by reacting 8-aza-9-acridone with phosphorus pentasulfide. Both substances are yielded as yellow needle crystalline substances, insoluble in alkalies and organic solvents and limitedly soluble in carbonate water solutions. Both of the substances may manifest prototropic (keto-enolic in A – C and thioketo-thioenolic tautomerism in D - F), which is confirmed by mass spectra (Figure 2):

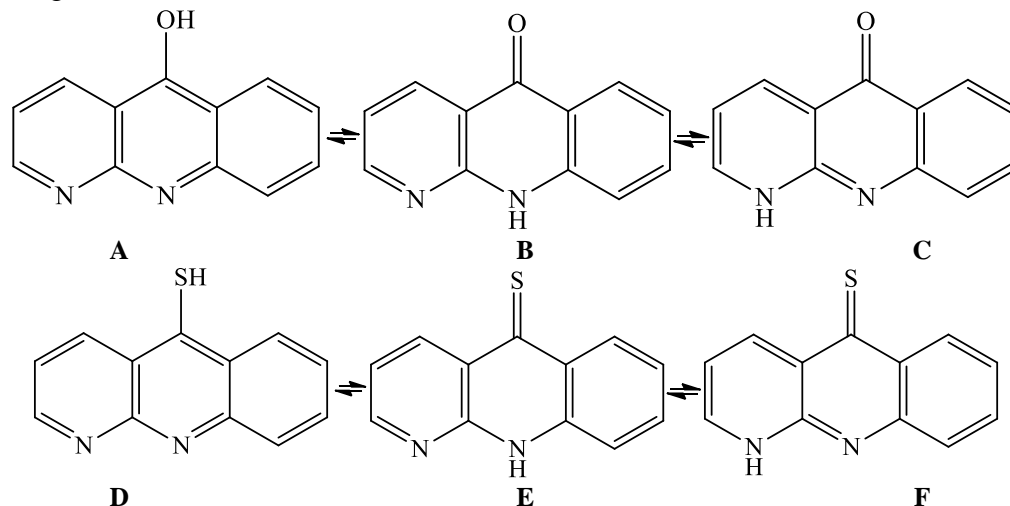


**Figure 2.** The tautomeric forms of the compounds 1 (A, B, C); 2 (D, E, F).

The mass spectrum of compound 1 contains the band of molecular ion  $[M]^+$  with  $m/z$  196. The isotope correction, equal to 14,23%, corresponds to the theoretically calculated (14,173%) for the molecular composition  $C_{12}H_8N_2O$ . The presence of three tautomers of the compound 1 may be proven by the IR spectrum (KBr), containing the absorbance bands of the bonds ( $cm^{-1}$ ):  $3400 = \nu_{NH}$  (broadband),  $3080 = \nu_{CH_{arom}}$ ,  $1700 = \nu_{C=O}$ ,  $1640 = \nu_{C=O}$  of pyridonic ring. The bands at 1610, 1540, and 1530 correspond to the bonds  $\nu_{C=C}$ ;  $\nu_{C=N}$ , and the bands at 1465, 1455, 1350, 1150, 1135, 770, 685 depict the  $\delta$ -oscillations of the hetaryl moiety. These data confirm the presence of forms B and C in the crystalline state of compound 1.

The mass spectrum confirms that the fragment CO leaves the structure of the molecular ion  $[M]^+$  (as 8-azacarbazolic derivative), confirming the presence of the structures B and C (the ion has  $m/z$  108). From the analysis of the mass-spectrum of metastable ions, it is possible to conclude that the ion with  $m/z$  167 is formed, which may be caused by either the direct C–OH elimination from  $[M]^+$  or with randomized hydrogen loss by the ion  $[M-CO]^+$ . In our case, it is impossible to estimate the content and impact of the enolic form A, which is very small, as  $J/M-CO^+ : J/M-COH^+$  ion intensity relation is nearly equal to 451, which confirms the presence of the forms B and C. The presence of the ions with  $m/z = 142 - / (M-CO) - C_2H_2^+$ ,  $m/z = 141 - / (M-CO) - HCN^+$  and  $m/z 140 - / (M-CO) - H_2CN^+$  indicates the possible presence of the tautomer B in the gas phase.

Therefore, the presence of all three tautomeric forms of compound 1 with the significant impact of the forms B and C is proven.

The mass-spectrum of the compound 1 (evaporation temperature  $85^\circ C$ ): 50/21/, 51/39/, 52/11/, 63/10/, 64/11/, 76/11/, 77/15/, 78/56/, 84/30/ –  $M-CO^{2+}$ , 92/10/, 98/12/ –  $/M^{2+}$ , 114/5/ –  $(M-CO)-HCN^+$ , 140/10/, 141/5/, 142/6/, 167/15/, 168/67/, 169/67/, 169/9/, 196/100 –  $/M^+$ , 197/14/.

The mass spectrum of compound 2 contains the peak  $/M^+$  with  $m/z$  212. The HRMS of this compound confirms its molar mass as equal to 212,0394, which corresponds to the brutto-formula  $C_{12}H_8N_2S$ , which confirms the correspondent structural formula.

As it is an acridonic analog, the thioacridone may exist in three tautomeric forms: D, E, and F. Nevertheless, the thiolic form of compound 2 is much more stable than compound 1, in which the impact of the molecular ions  $/M-H/^+$ ,  $/M-S/^+$  and  $/M-SH/^+$  is equal to 50%.

Therefore, compound 2 has three tautomers, the impacts of which are related as D:(E+F). The CS ion elimination confirms the presence of the forms E or F.  $/M-CS/^+$ , ion, as in 1, has an aza-carbazolic radical-cationic structure. The further ion decomposition is analogous to 1. The ion with  $m/z$  108 appears during the acridonic ring decomposition, which confirms the presence of the tautomer E or F.

The mass-spectrum of the compound 2 ( $t_{\text{evap}}=90^\circ\text{C}$ ),  $m/z$ : 50/10/, 51/23, 69/12/, 78/25/, 105,5/12/ -  $/M-H/^{2+}$ , 106/40/ -  $/M/^{2+}$ , 108/20/, 140/10/, 168/84/, 179/6/, 186/10/ -  $(M-HCN)^+$ , 211/88/, 212/100 -  $/M/^+$ , 213/14/.

The IR-spectrum of compound 2 reveals the absorbance bands (in  $\text{cm}^{-1}$ ), correspondent to  $3400 = \nu_{\text{NH}}$  (broadband), characterizing the form E or F,  $3020 = \nu_{\text{CH arom.}}$ ,  $2380 = \nu_{\text{SH}}$  (thiol D), 1630, 1600, 1540, 1560, 1500, 1440 corresponding to  $\nu_{\text{C=C}}$ ,  $\text{C=N}$  (8-aza acridine moiety),  $1240 = \nu_{\text{C=S}}$  (azathioacridone E or F).

Therefore, both IR and MS spectra confirm the presence of tautomeric forms and proton and electron delocalization. This also confirms the stability of radical-cation in different resonance forms, which favors the electropolymerization and chain propagation of both synthesized compounds, analogously to [22–27]. The electropolymerization will be given by positions 2 and 6 of the 8-aza-9-(thio)acridonic ring. For the anodic route, the polymerization potential of compound 2 will be lower than for compound 1 (especially in form D, compared to form A), as the thiolic group possesses more donating properties, which enhances the molecule electrophilicity.

The cathodic route, in which radical-anion acts as a chain initiator, is also possible, being more expressed for compound 1, in which the pyridonic moiety in the middle acts as an acceptor (Figure 3).

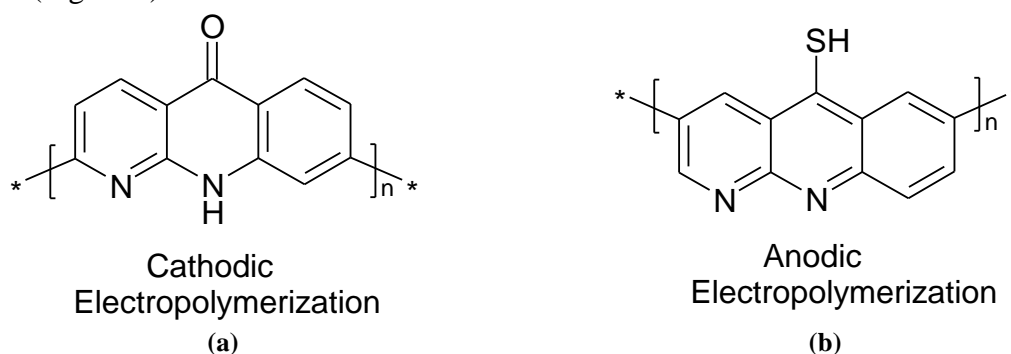


**Figure 3.** Conducting polymer structures for the (a) cathodically synthesized poly; (b) anodically synthesized poly.

Both polymeric forms may be excellent electrode modifiers for the electrochemical determination of biologically active compounds, as theoretically proven below. We chose ascorbic acid as dopamine as model compounds, as they are popular analytes for electroanalysis and biologically important [37–49]. Also, they describe the two-proton-two-electron leaving processes, including hydroquinone to quinone oxidation.

So, taking some assumptions [37–49] and considering that the ascorbic acid may either interact with the polymer or dope its active sites with the further electrooxidation within the polymer matrix, we describe the behavior of this system by the differential equation-set (1):

$$\begin{cases} \frac{da}{dt} = \frac{2}{\delta} \left( \frac{\Delta}{\delta} (a_0 - a) - r_a - r_d \right) \\ \frac{dh}{dt} = \frac{2}{\delta} \left( \frac{H}{\delta} (h_0 - h) - r_h \right) \\ \frac{dp}{dt} = \frac{1}{P} (r_a + r_d + r_h - r_o) \end{cases} \quad (1)$$

Herein,  $\Delta$  and  $H$  are ascorbic acid and dopamine diffusion coefficients,  $a_0$  and  $h_0$  their bulk concentrations,  $a$  and  $h$  their pre-surface concentrations,  $\delta$  is the diffusion layer thickness,  $p$  is the modified poly(1) or poly(2) surface coverage degree,  $P$  is its maximal surface concentration and the parameters  $r$  stand for the correspondent reaction rates, calculated as (2 – 5):

$$r_a = k_a a (1 - p) \quad (2)$$

$$r_d = k_d a^x (1 - p) \exp\left(\frac{nF\varphi_0}{RT}\right) \quad (3)$$

$$r_h = k_h h (1 - p) \quad (4)$$

$$r_o = k_o p \exp\left(\frac{xF\varphi_0}{RT}\right) \quad (5)$$

Herein, the parameters  $k$  stand for the correspondent reaction rate constants,  $x$  is the ascorbic acid polymer doping reaction order,  $n$ , and  $x$  are the numbers of electrons transferred during the doping and oxidative regeneration of the polymer,  $F$  is the Faraday number,  $\varphi_0$  stands for zero-charge-related potential slope,  $R$  is the ideal gas constant, and  $T$  is the absolute temperature.

The doping of the ascorbic acid may be realized by either cation-radical sites or the pyridinic nitrogen atoms (its realization depends on the solution pH and on the tautomeric form by which the polymer is formed), and it may influence the polymer conductivity. Nevertheless, this influence won't negatively impact the electroanalytical activity of the polymer of the novel 8-azaacridinic compounds, as the steady-state stability condition is satisfied in a vast concentration range for both analytes, as shown below.

### 3. Results and Discussion

In order to investigate the electroanalytical process of dopamine and ascorbic acid determination by the polymer of the novel aza acridinic compound, we analyze the steady-state stability of the equation-set (1) and expose the Jacobian determinant as (6):

$$\begin{pmatrix} a_{11} & a_{12} & a_{13} \\ a_{21} & a_{22} & a_{23} \\ a_{31} & a_{32} & a_{33} \end{pmatrix} \quad (6)$$

In which:

$$a_{11} = \frac{2}{\delta} \left( -\frac{\Delta}{\delta} - k_a (1 - p) - x k_d a^{x-1} (1 - p) \exp\left(\frac{nF\varphi_0}{RT}\right) \right) \quad (7)$$

$$a_{12} = 0 \quad (8)$$

$$a_{13} = \frac{2}{\delta} \left( k_a a + k_d a^x \exp\left(\frac{nF\varphi_0}{RT}\right) - j k_d a^x (1 - p) \exp\left(\frac{nF\varphi_0}{RT}\right) \right) \quad (9)$$

$$a_{21} = 0 \quad (10)$$

$$a_{22} = \frac{2}{\delta} \left( -\frac{H}{\delta} - k_h (1 - p) \right) \quad (11)$$

$$a_{23} = \frac{2}{\delta} (k_d h) \quad (12)$$

$$a_{31} = \frac{1}{P} \left( k_a (1 - p) + x k_d a^{x-1} (1 - p) \exp\left(\frac{nF\varphi_0}{RT}\right) \right) \quad (13)$$

$$a_{32} = \frac{1}{P} (k_d (1 - p)) \quad (14)$$

$$a_{33} = \frac{1}{p} \left( -k_a a - k_a a^x \exp\left(\frac{nF\varphi_0}{RT}\right) + jk_a a^x (1-p) \exp\left(\frac{nF\varphi_0}{RT}\right) - k_d h - k_o \exp\left(\frac{xF\varphi_0}{RT}\right) + jk_o p \exp\left(\frac{xF\varphi_0}{RT}\right) \right) \quad (15)$$

In terms of the *oscillatory behavior*, this system will resemble the simplest case. Still, the oscillatory behavior will be more probable, as the double electric layer and surface ionic force, conductivity, and impedance will be affected by two electrochemical stages instead of only one for the simplest case.

The Hopf bifurcation, correspondent to the oscillatory behavior, is realized if the main diagonal elements (7), (11), and (15) contain the positive elements, describing the positive callback. Only one of them (15) possesses two of those elements, which are  $jk_a a^x (1-p) \exp\left(\frac{nF\varphi_0}{RT}\right)$  and  $jk_o p \exp\left(\frac{xF\varphi_0}{RT}\right)$ , positive if  $j > 0$ , each one corresponds to the del ionic force cyclic changes by each one of the electrochemical processes. The oscillations are expected to be frequent and of small amplitude.

Simplifying the expressions during the determinant analysis, we introduce new variables, rewriting the determinant as (16):

$$\frac{4}{\delta^2} \begin{vmatrix} -\xi - \Sigma & 0 & -T \\ 0 & -\lambda - \Lambda & -P \\ \Sigma & \Lambda & -T - P - \Omega \end{vmatrix} \quad (16)$$

Considering that:

$$-Det J \begin{cases} > 0, \text{ for steady - state stability} \\ = 0 \text{ monotonic instability} \end{cases} \quad (17)$$

Opening the brackets and considering the requisite  $-Det J > 0$ , salient from the criterion, we obtain the steady-state stability and monotonic instability (detection limit) conditions, expressed as:

$$\xi(\lambda T + \Lambda T + \lambda P + \lambda \Omega + \Lambda \Omega) + \Sigma(\lambda T + \lambda P + \lambda \Omega + \Lambda \Omega) \begin{cases} > 0, \text{ linear concentration range} \\ = 0, \text{ detection limit} \end{cases} \quad (18)$$

If  $-Det J > 0$ , the Routh-Hurwitz stability criterion is valid, and the steady-state is thereby stable, providing an efficient electrochemical detection of both substances. Moreover, although the stability region is narrower than in similar systems [47–49], it even lets us use this system as an electroanalytical for sensing purposes due to the efficient analytical signal interpretation. The electroanalytical process is both diffusion and kinetically controlled.

The condition  $Det J = 0$  corresponds to the detection limit, manifested by the *monotonic instability*. It may be seen as an N-shaped part of the steady-state voltammogram, depicts the margin between stable and unstable states, and corresponds to steady-state multiplicity. In other words, multiple steady-states, each one unstable, coexist at this point.

The system's behavior becomes more dynamic if a chlorogenic analyte, like sucralose, is used. It is analogous to that described in the article [47] for the anodic process and [48] for the cathodic.

#### 4. Conclusions

Two novel aza acridinic derivatives have been synthesized and characterized. The IR and MS analysis has confirmed the possibility of tautomeric transformations, which facilitate electropolymerization by both cathodic and anodic routes. The analysis of the mathematical model for the use of conducting polymer for each of these compounds for ascorbic acid and dopamine electrochemical determination confirms its efficiency as an electrode modifier.

## Funding

This research received no external funding.

## Acknowledgments

Volodymyr V. Tkach acknowledges the Engineering Faculty of the University of Porto and the University of Trás-os-Montes and Alto Douro for their support during these difficult times for Ukraine and its research.

## Conflicts of Interest

The authors declare no conflict of interest.

## References

1. Elebiju, O.F.; Ajani, O.O.; Oduselu, G.O.; Ogunnupebi, T.A.; Adebisi, E. Recent advances in functionalized quinoline scaffolds and hybrids—Exceptional pharmacophore in therapeutic medicine. *Front. Chem.* **2023**, *10*, 1074331, <https://doi.org/10.3389/fchem.2022.1074331>.
2. Chauhan, S.; Umar, T.; Aulakh, M.K. Quinolines: Privileged Scaffolds for Developing New Anti-neurodegenerative Agents. *ChemistrySelect* **2023**, *8*, e202204960, <https://doi.org/10.1002/slct.202204960>.
3. Shehi, V.; Verma, H.; Saha, S.; Kumar, S.; Pathak, D. An Extensive Review on Biological Interest of Quinoline and Its Analogues. *Int. J. Sci. Healthcare Res.* **2023**, *8*, 45–66, <https://doi.org/10.52403/ijshr.20230105>.
4. Dine, I.; Mulugeta, E.; Melaku, Y.; Belete, M. Recent advances in the synthesis of pharmaceutically active 4-quinolone and its analogues: a review. *RSC Adv.* **2023**, *13*, 8657–8682, <https://doi.org/10.1039/d3ra00749a>.
5. Różycka, D.; Kowalczyk, A.; Denel-Bobrowska, M.; Kuźmycz, O.; Gapińska, M.; Stączek, P.; Olejniczak, A.B. Acridine/Acradone–Carborane Conjugates as Strong DNA-Binding Agents with Anticancer Potential. *ChemMedChem* **2023**, *18*, e202200666, <https://doi.org/10.1002/cmde.202200666>.
6. Al-Khafaji, M.K.; Al-Yasari, A.; Mohammed, A.I. A Theoretical Molecular Design of Acridine/Anthracene Polyoxometalate Hybrid Materials for Enhanced Dye-Sensitized Solar Cells Performance. *ChemistrySelect* **2023**, *8*, e202302230, <https://doi.org/10.1002/slct.202302230>.
7. Fornaciari, B.; Juvenal, M.S.; Martins, W.K.; Junqueira, H.C.; Baptista, M.S. Photodynamic Activity of Acridine Orange in Keratinocytes under Blue Light Irradiation. *Photochem* **2023**, *3*, 209–226, <https://doi.org/10.3390/photochem3020014>.
8. Nowak, P.; Sikorski, A. Structural diversity of cocrystals formed from acridine and two isomers of hydroxybenzaldehyde: 3-hydroxybenzaldehyde and 4-hydroxybenzaldehyde. *RSC Adv.* **2023**, *13*, 20105–20112, <https://doi.org/10.1039/d3ra02300a>.
9. Islam, M.B.; Islam, M.I.; Nath, N.; Emran, T.B.; Rahman, M.R.; Sharma, R.; Matin, M.M. Recent Advances in Pyridine Scaffold: Focus on Chemistry, Synthesis, and Antibacterial Activities. *BioMed Res. Int.* **2023**, *2023*, 9967591, <https://doi.org/10.1155/2023/9967591>.
10. Imtiaz, S.; Singh, B.; Khan, M.M. Chapter 10 - Synthesis of pyridine derivatives using multicomponent reactions. In *Recent Developments in the Synthesis and Applications of Pyridines*, Singh, P., Ed.; Elsevier, **2023**; 299–330, <https://doi.org/10.1016/b978-0-323-91221-1.00006-3>.
11. Maity, S.; Bera, A.; Bhattacharjya, A.; Maity, P. C–H functionalization of pyridines. *Org. Biomol. Chem.* **2023**, *21*, 5671–5690, <https://doi.org/10.1039/d3ob00799e>.
12. Rieffer, J.; Zapf, L.; Wirthensohn, R.; Hennig, P.T.; Ribbeck, T.; Sprenger, J.A.P.; Ignat'ev, N.V.; Finze, M. Pyridine Adducts of Tricyano- and Dicyanoboranes. *Eur. J. Org. Chem.* **2023**, *26*, e202300031, <https://doi.org/10.1002/ejoc.202300031>.
13. Hosu, O.; Barsan, M.M.; Săndulescu, R.; Cristea, C.; Brett, C.M.A. Hybrid Nanocomposite Platform, Based on Carbon Nanotubes and Poly(Methylene Blue) Redox Polymer Synthesized in Ethaline Deep Eutectic Solvent for Electrochemical Determination of 5-Aminosalicylic Acid. *Sensors* **2021**, *21*, 1161, <https://doi.org/10.3390/s21041161>.

14. Yin, C.; Zhuang, Q.; Xiao, Q.; Wang, Y.; Xie, J. Electropolymerization of poly(methylene blue) on flower-like nickel-based MOFs used for ratiometric electrochemical sensing of total polyphenolic content in chrysanthemum tea. *Anal. Methods* **2021**, *13*, 1154–1163, <https://doi.org/10.1039/d1ay00028d>.
15. Farias, E.A.d.O.; Furtado, N.J.S.; Macêdo, I.Y.L.d.; Gil, E.d.S.; Guimarães, F.F.; Bastos, R.S.; Rocha, J.A.; Nunes, L.C.C.; Luz, R.A.d.S.; Eiras, C. Poly(Alizarin Red S) on pyrolytic graphite electrodes as a new multi-electronic system for sensing oxandrolone in urine. *Biosens. Bioelectron.* **2021**, *185*, 113234, <https://doi.org/10.1016/j.bios.2021.113234>.
16. Al-Jawadi, E.A.M.; Majeed, M.I. Detection of anticancer drug by electrochemical sensors at Modified Electrode (MWCNT/polyEosin-Y). *Nanomed. Res. J.* **2021**, *6*, 50–59, <https://doi.org/10.22034/NMRJ.2021.01.006>.
17. Isik, H.; Öztürk, G.; Ağin, F.; Kul, D. Electroanalytical Analysis of Guaifenesin on Poly(Acridine Orange) Modified Glassy Carbon Electrode and its Determination in Pharmaceuticals and Serum Samples. *Comb. Chem. High Throughput Screen.* **2021**, *24*, 376–385, <https://doi.org/10.2174/1386207323666200709170450>.
18. Monnappa, A.B.; Manjunatha, J.G.G.; Bhatt, A.S.; Nagarajappa, H. Sensitive and selective electrochemical detection of vanillin at graphene based poly (methyl orange) modified electrode. *J. Sci.: Adv. Mater. Devices* **2021**, *6*, 415-424, <https://doi.org/10.1016/j.jsamd.2021.05.002>.
19. Liv, L. A facile poly(allura red) film for signal-amplified electrochemical sensing of dopamine and uric acid in human plasma and urine. *Microchem. J.* **2023**, *195*, 109425, <https://doi.org/10.1016/j.microc.2023.109425>.
20. Liv, L.; Portakal, M.; Çukur, M.S.; Topaçlı, B.; Uzun, B. Electrocatalytic Determination of Uric Acid with the Poly(Tartrazine)-Modified Pencil Graphite Electrode in Human Serum and Artificial Urine. *ACS Omega* **2023**, *38*, 34420–34430, <https://doi.org/10.1021/acsomega.3c02561>.
21. Kulikova, T.; Porfireva, A.; Rogov, A.; Evtugyn, G. Electrochemical DNA Sensor Based on Acridine Yellow Adsorbed on Glassy Carbon Electrode. *Sensors* **2021**, *21*, 7763, <https://doi.org/10.3390/s21227763>.
22. Akkapinyo, C.; Subannajui, K.; Poo-arporn, Y.; Poo-arporn, R.P. Disposable Electrochemical Sensor for Food Colorants Detection by Reduced Graphene Oxide and Methionine Film Modified Screen Printed Carbon Electrode. *Molecules* **2021**, *26*, 2312, <https://doi.org/10.3390/molecules26082312>.
23. Tajik, S.; Orooji, Y.; Ghazanfari, Z.; Karimi, F.; Beitollahi, H.; Varma, R.S.; Jang, H.W.; Shokouhimehr, M. Nanomaterials modified electrodes for electrochemical detection of Sudan I in food. *J. Food Meas. Charact.* **2021**, *15*, 3837-3852, <https://doi.org/10.1007/s11694-021-00955-1>.
24. Neupane, S.; Bhusal, S.; Subedi, V.; Nakarmi, K.B.; Gupta, D.K.; Yadav, R.J.; Yadav, A.P. Preparation of an Amperometric Glucose Biosensor on Polyaniline-Coated Graphite. *J. Sensors* **2021**, *2021*, 8832748, <https://doi.org/10.1155/2021/8832748>.
25. Feng, X.; Sun, S.; Cheng, G.; Shi, L.; Yang, X.; Zhang, Y.; Rangabhashiyam, S. Removal of Uranyl Ion from Wastewater by Magnetic Adsorption Material of Polyaniline Combined with CuFe<sub>2</sub>O<sub>4</sub>. *Adsorpt. Sci. Technol.* **2021**, *2021*, 5584158, <https://doi.org/10.1155/2021/5584158>.
26. McDaniel, J.G.; Josowicz, M.; Janata, J. Cover Feature: Quantized Electrodes: Atomic Palladium and Gold in Polyaniline (ChemElectroChem 10/2021). *ChemElectroChem* **2021**, *8*, 1696, <https://doi.org/10.1002/celec.202100428>.
27. Falletta, E.; Ferretti, A.M.; Mondini, S.; Evangelisti, C.; Capetti, E.; Olivetti, E.S.; Martino, L.; Beatrice, C.; Soares, G.; Pasquale, M.; Della Pina, C.; Ponti, A. Size-dependent catalytic effect of magnetite nanoparticles in the synthesis of tunable magnetic polyaniline nanocomposites. *Chem. Pap.* **2021**, *75*, 5057-5069, <https://doi.org/10.1007/s11696-021-01604-z>.
28. Tesfaye, G.; Hailu, T.; Ele, E.; Negash, N.; Tessema, M. Square wave voltammetric determination of quercetin in wine and fruit juice samples at poly (safranin O) modified glassy carbon electrode. *Sens. Bio-Sens. Res.* **2021**, *34*, 100466, <https://doi.org/10.1016/j.sbsr.2021.100466>.
29. Ziyatdinova, G.; Yakupova, E.; Zhupanova, A. Voltammetric Sensors Based on the Electropolymerized Phenolic Acids or Triphenylmethane Dyes for the Antioxidant Analysis. *Eng. Proc.* **2022**, *27*, 2, <https://doi.org/10.3390/ecsa-9-13178>.
30. Huang, J.; Zhang, T.; Dong, G.; Zhu, S.; Yan, F.; Liu, J. Direct and Sensitive Electrochemical Detection of Bisphenol A in Complex Environmental Samples Using a Simple and Convenient Nanochannel-Modified Electrode. *Front. Chem.* **2022**, *10*, 900282, <https://doi.org/10.3389/fchem.2022.900282>.

31. Yuan, J.; Huang, B.; Lu, Y.; Jiang, L.; He, G.; Chen, H. Ultrasensitive electrochemical detection of bisphenol A using composites of MoS<sub>2</sub> nanoflowers, CoS<sub>2</sub> nano-polyhedrons and reduced graphene oxide. *Environ. Chem. Lett.* **2022**, *20*, 2751–2756, <https://doi.org/10.1007/s10311-022-01442-9>.
32. Mercante, L.A.; Iwaki, L.E.O.; Scagion, V.P.; Oliveira, O.N., Jr.; Mattoso, L.H.C.; Correa, D.S. Electrochemical Detection of Bisphenol A by Tyrosinase Immobilized on Electrospun Nanofibers Decorated with Gold Nanoparticles. *Electrochem* **2021**, *2*, 41–49, <https://doi.org/10.3390/electrochem2010004>.
33. Zhu, X.; Wang, X.; Li, N.; Wang, Q.; Liao, C. Bioelectrochemical system for dehalogenation: A review. *Environ. Pollut.* **2022**, *293*, 118519, <https://doi.org/10.1016/j.envpol.2021.118519>.
34. Joshi, N.C.; Malik, S.; Gururani, P. Utilization of Polypyrrole/ZnO Nanocomposite in the Adsorptive Removal of Cu<sup>2+</sup>, Pb<sup>2+</sup> and Cd<sup>2+</sup> Ions from Wastewater. *Lett. Appl. NanoBioSci.* **2021**, *10*, 2339–2351, <https://doi.org/10.33263/LIANBS103.23392351>.
35. Cantillo, D. Synthesis of active pharmaceutical ingredients using electrochemical methods: keys to improve sustainability. *Chem. Commun.* **2022**, *58*, 619–628, <https://doi.org/10.1039/D1CC06296D>.
36. Nazari, Z.; Hadi Nematollahi, M.; Zareh, F.; Pouramiri, B.; Mehrabani, M. An Electrochemical Sensor Based on Carbon Quantum Dots and Ionic Liquids for Selective Detection of Dopamine. *ChemistrySelect* **2023**, *8*, e202203630, <https://doi.org/10.1002/slct.202203630>.
37. Delmo, N.; Mostafiz, B.; Ross, A.E.; Suni, J.; Peltola, E. Developing an electrochemical sensor for the *in vivo* measurements of dopamine. *Sens. Diagn.* **2023**, *2*, 559–581, <https://doi.org/10.1039/d2sd00230b>.
38. Alahmadi, N.; El-Said, W.A. Electrochemical Sensing of Dopamine Using Polypyrrole/Molybdenum Oxide Bilayer-Modified ITO Electrode. *Biosensors* **2023**, *13*, 578, <https://doi.org/10.3390/bios13060578>.
39. Javed, A.; Fatima, B.; Hussain, D.; Zahra Jawad, S.E.; Subhan, M.; Najam-ul-Haq, M. Effect of narcotic drugs on neurotransmitter: Electrochemical determination of heroin and dopamine by graphene oxide/carboxymethylcellulose/magnesium oxide nanohybrid membrane. *J. Mol. Liq.* **2023**, *384*, 122154, <https://doi.org/10.1016/j.molliq.2023.122154>.
40. Ankitha, M.; Shabana, N.; Mohan Arjun, A.; Muhsin, P.; Abdul Rasheed, P. Ultrasensitive electrochemical detection of dopamine from human serum samples by Nb<sub>2</sub>CT<sub>x</sub>MoS<sub>2</sub> hetero structures. *Microchem. J.* **2023**, *187*, 108424, <https://doi.org/10.1016/j.microc.2023.108424>.
41. Sato, N.; Ohta, Y.; Haruta, M.; Takehara, H.; Tashiro, H.; Sasagawa, K.; Jongprateep, O.; Ohta, J. Electrochemical activities of Fe<sub>2</sub>O<sub>3</sub>-modified microelectrode for dopamine detection using fast-scan cyclic voltammetry. *AIP Adv.* **2023**, *13*, 025026, <https://doi.org/10.1063/5.0123865>.
42. Muqaddas, S.; Aslam, H.; Ul Hassan, S.; Raza Ashraf, A.; Adeel Asghar, M.; Ahmad, M.; Nazir, A.; Shoukat, R.; Kaleli, M.; Mostafa Ibrahim, S.; kyürekli, S.; Haider, A.; Ali, A. Electrochemical sensing of glucose and ascorbic acid via POM-based CNTs fiber electrode. *Mater. Sci. Eng. B* **2023**, *293*, 116446, <https://doi.org/10.1016/j.mseb.2023.116446>.
43. Dodevska, T.; Hadzhiev, D.; Shterev, I. A Review on Electrochemical Microsensors for Ascorbic Acid Detection: Clinical, Pharmaceutical, and Food Safety Applications. *Micromachines* **2023**, *14*, 41, <https://doi.org/10.3390/mi14010041>.
44. Alberti, G.; Zaroni, C.; Magnaghi, L.R.; Biesuz, R. Ascorbic Acid Sensing by Molecularly Imprinted Electrosynthesized Polymer (e-MIP) on Screen-Printed Electrodes. *Chemosensors* **2023**, *11*, 348, <https://doi.org/10.3390/chemosensors11060348>.
45. Mirzaei Karazan, Z.; Roushani, M. Electrochemical Sensor Based on Molecularly Imprinted Copolymer for Selective and Simultaneous Determination of Ascorbic Acid and Tyrosine. *Anal. Bioanal. Chem. Res.* **2023**, *10*, 269–278, <https://doi.org/10.22036/abcr.2023.376925.1863>.
46. Ma, T.; Wang, Y.; Hasebe, Y.; Zhang, Z. A Carbon-Black Doped Molybdenite-Based Electrochemical Sensor for Simultaneous Determination of Uric Acid, Dopamine and Ascorbic Acid. *ChemistrySelect* **2023**, *8*, e202300226, <https://doi.org/10.1002/slct.202300226>.
47. Tkach, V.V.; Storoshchuk, N.M.; Oliveira, S.C.d.; Ivanushko, Y.G.; Nazymok, Y.V.; Luganska, O.V.; Yagodynets, P.I. The theoretical description for the sucralose electrochemical determination, assisted by poly(safranin) modified electrode. *Ukr. Bioorg. Acta* **2021**, *16*, 34–37, <https://doi.org/10.15407/bioorganica2021.02.034>.
48. Tkach, V.V.; Storoshchuk, N.M.; Storoshchuk B.D.; de Oliveira, S.C.; Ivanushko, Y.G.; Kryvetskyi, V.V.; Kryvetska, I.I.; Kryvetskyi, I.V.; Yemelienenko, N.R.; Narsiia, V.I.; Yagodynets, P.I.; da Silva, A.O.; Masna, Z.Z.; Shevchenko, I.M.; Gnitsevych, V.A.; Medvedeva, A.O.; Vasylieva, O.O.; Musayeva, D.M.; Kosimov, X.; Jabborova, O.; Samadov, B.; Sagdullayeva, G.; Hamdanova, G.; Karputina, M.V.; Khargelia,

- D.D.; Garcia, J.R.; Odyntsova, V.M.; da Paiva Martins, J.I.F. The Theoretical Description of Sucralose Cathodic Electrochemical Determination over a Poly(safranin) Modified Electrode in Acidic Media. *Biointerface Res. Appl. Chem.* **2023**, *13*, 520, <https://doi.org/10.33263/BRIAC136.520>.
49. Tkach, V.V.; Kushnir, M.V.; Storoshchuk, N.M.; de Oliveira, S.C.; Luganska, O.V.; Kopiika, V.V.; Novosad, N.V.; Lukanova, S.M.; Ivanushko, Y.G.; Ostapchuk, V.G.; Melnychuk, S.P.; Yagodynets', P.I.; da Paiva Martins, J.I.F.; dos Reis, L.V. O uso do hidróxido de vanádio bivalente para a eliminação da sucralose das águas naturais e de esgoto da indústria alimentar e farmacêutica. Uma avaliação teórica. *Rev. Colomb. Cienc. Quím.-Farm.* **2023**, *52*, 348–361, <https://doi.org/10.15446/rcciquifa.v52n2.110749>.